RevMexAA (Serie de Conferencias), **37**, 83–93 (2009)

MULTI-WAVELENGTH MODELLING OF DUSTY GALAXIES. GRASIL AND APPLICATIONS

L. Silva[1]

RESUMEN

La distribución espectral de energía de galaxias contiene la información convolucionada de su contenido estelar y gaseoso y de la tasa e historia de su formación estelar. Es por consiguiente un sondeo esencial de las propiedades galácticas. Cada intervalo espectral está mayormente dominado por determinadas fuentes específicas de emisión o por procesos radiativos tales que únicamente modelando todo el intervalo espectral es posible deconvolucionar e interpretar la información contenida en la SED en términos de la SFR y de la evolución en general. Los ingredientes y los métodos de computación considerados en modelos de las SEDs en galaxias dependen de la motivación. Los modelos teóricos tienen una ventaja sobre los modelos semi-empíricos observacionalmente calibrados en razón a su capacidad de interpretar y predecir resultados a pesar de involucrar mayor tiempo de cómputo. Resumo aquí las características del código `GRASIL` para calcular las SEDs de galaxias desde el UV hasta el radio tratando con especial cuidado el tranporte radiativo y la emisión del polvo. El código ha sido extensamente aplicado para interpretar observaciones y hacer predicciones para modelos semi-analíticos de formación de galaxias. Presento en particular las aplicaciones en el contexto de modelos de galaxias y el nuevo método implementado en `GRASIL` basado en el algoritmo de redes neuronales artificiales para lidiar con el tiempo de cómputo en aplicaciones cosmológicas

ABSTRACT

The spectral energy distribution of galaxies contains a convolved information on their stellar and gas content, on the star formation rate and history. It is therefore the most direct probe of galaxy properties. Each spectral range is mostly dominated by some specific emission sources or radiative processes so that only by modelling the whole spectral range it is possible to de-convolve and interpret the information contained in the SED in terms of SFR and galaxy evolution in general. The ingredients and kind of computations considered in models for the SEDs of galaxies depend on their aims. Theoretical models have the advantage of a broader interpretative and predictive power with respect to observationally calibrated semi-empirical approaches, the major drawback being a longer computational time. I summarize the main features of `GRASIL`, a code to compute the UV to radio SED of galaxies treating the radiative transfer and dust emission with particular care. It has been widely applied to interpret observations and to make predictions for semi-analytical galaxy formation models. I present in particular the applications in the context of galaxy models, and the new method implemented in `GRASIL` based on the artificial neural network algorithm to cope with the computing time for cosmological applications.

Key Words: galaxies: evolution — galaxies: ISM — infrared: galaxies — ISM: dust, extinction — radiative transfer

1. INTRODUCTION

1.1. *SED components*

The spectral energy distribution (SED) of galaxies contains a convolved information on their stellar and gas content, on the age and abundances of stellar populations, on the chemistry and physical state of the interstellar medium (ISM), on the star formation rate (SFR) and history. It is therefore the most direct probe of galaxy properties. Each spectral range is mostly dominated by some specific emission sources or radiative processes acting on different time scales, so that only by possibly analysing/predicting the whole spectral range one can hope to de-convolve and interpret the information contained in the SED in terms of SFR and galaxy evolution in general.

The different components are schematically shown in Figure 1. The energy emitted by stars mainly in the UV/optical to NIR spectral range is the result of the star formation history/mass assembly underwent by galaxies and giving rise to the specific mixture of ages, metallicity and mass distribution of the stellar populations. This emission interacts with gas and dust in the ISM before emerging from galaxies. UV photons ionize and excite the

[1]INAF/Trieste, Via Tiepolo 11, I-34121, Trieste, Italy (silva@oats.inaf.it).

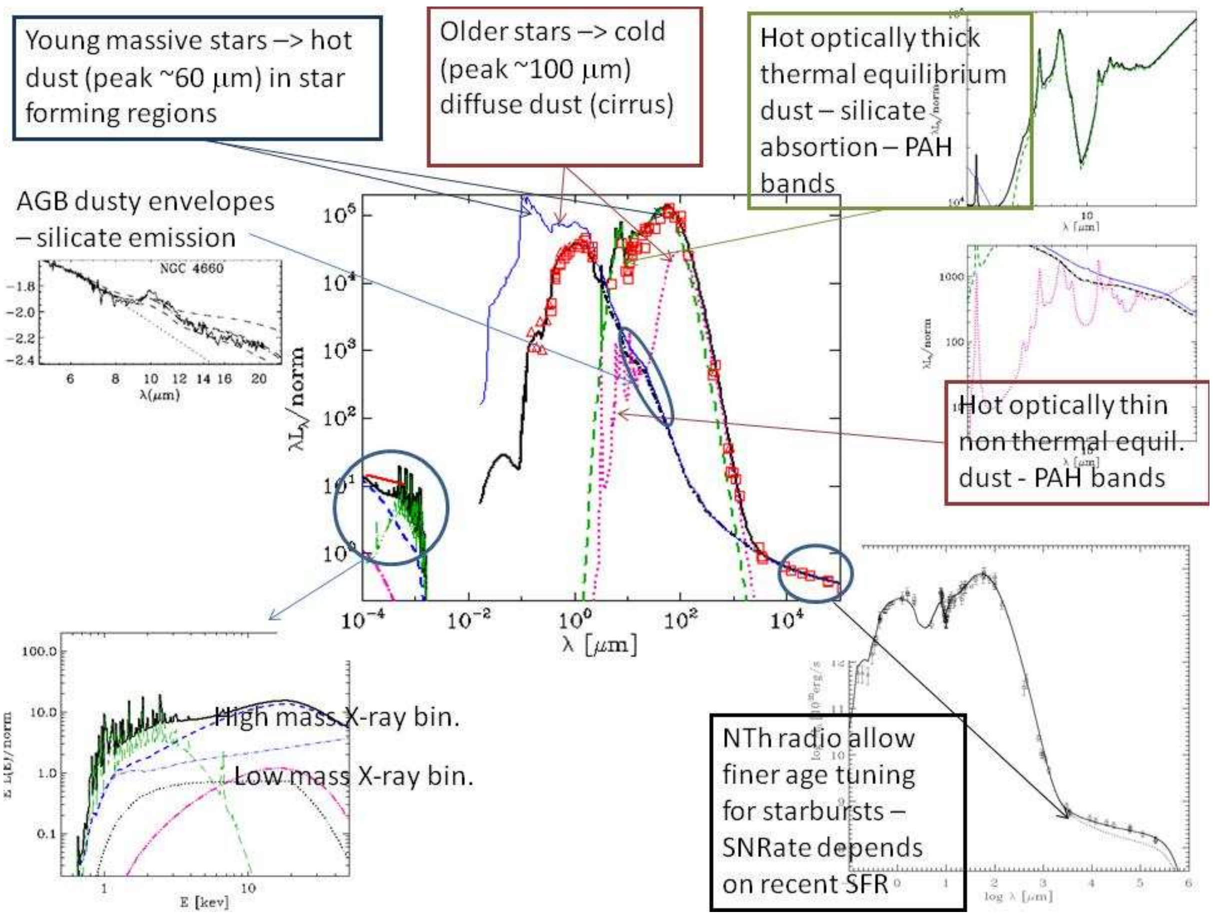

Fig. 1. Schematic summary of the sources mostly contributing to the different spectral ranges. The central plot shows a model fitting M82 as an example. The emission $\lesssim 3000$ Å is dominated by young massive stars. In most cases a large fraction of this energy is absorbed by dust in optically thick star forming regions and re-emitted as relatively hot mid and far IR emission. The energy from more evolved stars, mostly emitting in the optical and near-IR, interacts with the diffuse ISM. The absorbed fraction is re-emitted as cooler thermal radiation peaking at ~ 100 μm. The mid-IR continuum originates from hot dust both in thermal equilibrium with the radiation field and from very small grains fluctuating in temperature after the absorption of single UV photons. The mid-IR features reveal the thickness and composition of the dust (depth of the 9.7 μm silicate feature, and PAH emission bands). In quiescent or post-starburst galaxies, the dust emission from AGB (ages $\sim 10^8$ yr to a few Gyrs) circumstellar envelopes can dominate the mid-IR (Bressan et al. 1998, 2006). The hard X-ray ($\gtrsim 2$ keV) emission in star-forming galaxies originates from X-ray binaries, with high-mass systems (mass of the secondary $\gtrsim 8$ $M_\odot$) dominating in starburst galaxies, and low-mass systems (mass of the secondary ~ 1 $M_\odot$) dominating in normal star forming galaxies. The non-thermal radio emission is explained as synchrotron radiation from electrons injected into the ISM by supernovae explosions, and accelerated by the galactic magnetic field. It is therefore related to the recent SFR and together with the IR allows a finer age tuning, e.g. in a starburst the IR follows the SFR without delay while the radio emission needs at least the explosion of the first SNae to occur (Bressan et al. 2002). See text for more details.

gas producing HII regions with emission lines, that are probes of the SFR and the chemistry, energetics and physical state of the ISM where they are produced. Atomic and molecular lines are present from the X-ray to the radio range originating from electronic or rotational/vibrational transitions. The radio energy is mainly explained with free-free emission from ionized nebulae and synchrotron radiation by supernova-injected electrons accelerated by the galaxy magnetic field. The X-ray range probes mainly the emission from hot plasma and from X-ray binary stars. The SED from a few μm to the sub-mm (generally IR) is dominated by dust emission after interaction with stellar radiation. Dust in

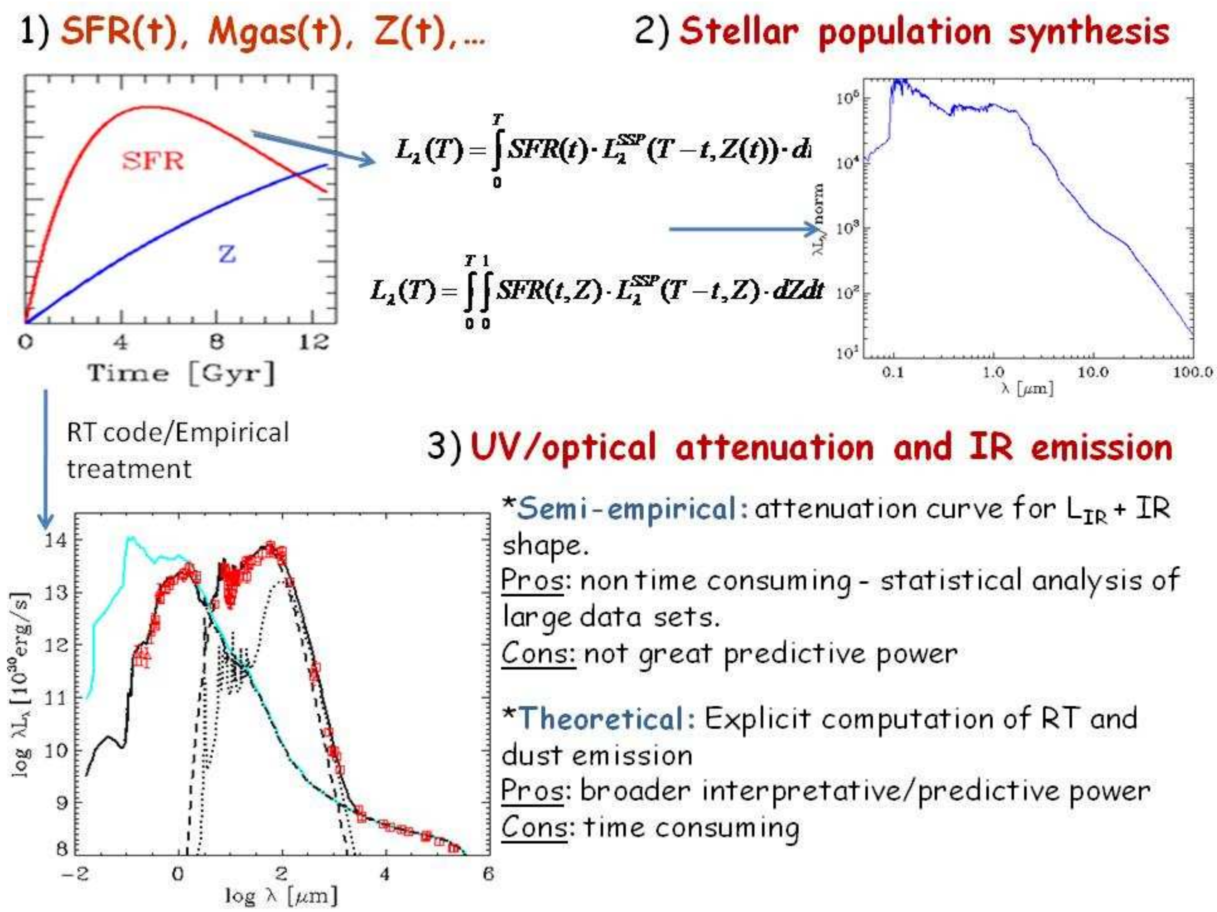

Fig. 2. Schematic description of the main ingredients and relative aims of models for the SEDs of galaxies: (1) Star formation history and possibly the corresponding evolution of the mass of gas and metallicity, and of other galaxy properties. These inputs are obtained either with simple exponentials, or more detailed chemical evolution models, or galaxy formation models. (2) Library of SSP spanning a wide range in age and metallicity. The sum of the spectral luminosity contributed by the stellar generations born at each time step, weighted by the SFR at their birth, provides the pure stellar integrated SEDs. (3) The ways in which the UV/optical attenuation and IR dust emission are usually treated can be broadly classified into two main groups, semi-empirical and theoretical. In semi-empirical approaches, an attenuation law is adopted (e.g. Calzetti 2000; Charlot & Fall 2000, or an extinction curve with a slab geometry etc). This provides also the IR luminosity, whose shape is assigned with modified black-body curves or templates with different relative normalizations typically calibrated on observed IR colors. These very fast methods are useful in particular for statistical analysis of large data sets, but may lack predictive power. In theoretical models an explicit evaluation of the extinction and dust emission is performed, with different levels of complexities and approximations, depending also on the aims. In this way the effective input SF history, mass of gas and geometrical information, if available, are accounted for. These models have more predictive power to test not well observed (high-z) galaxies or different assumptions, but may require too long computing times.

galaxies, although being a small fraction of the mass of gas (~ 0.01 in our Galaxy), is a fundamental ingredient occurring in many environments –such as circumstellar envelopes, supernova remnants, star-forming regions and diffuse clouds– and intervening and affecting many chemical and physical processes, for instance by acting as a catalyst for the formation of H_2 molecules, by shielding dense and cold regions from photo-dissociating UV photons allowing gravitational collapse and star formation, by driving mass-loss in evolved stars, by depleting heavy elements from the gas phase (e.g. Mathis 1990; Dorschner & Henning 1995; Draine 2003). Dust grains absorb and scatter short wavelength radiation ($\lambda \lesssim 1\mu$m) with high efficiency and emit thermally the absorbed energy in the IR where the extinction efficiency steeply drops, because the sublimation temperature of dust is typically ~ 1500 K, therefore dust shapes the SED of galaxies.

1.2. *Model ingredients and aims*

The modelling of the entire SED of galaxies is therefore very complex and full of uncertainties. Because of this different approaches have been proposed, depending also on the purpose of the applications. A general broad scheme of the ingredients and relative aims is shown in Figure 2:

• A first input to provide, if accounting for the evolution of the stellar populations, is the star formation history, and possibly the corresponding evolution of the metallicity, of the mass of gas and dust etc. These quantities are typically obtained by adopting simple exponentials with different e-folding time scales, or more complete chemical evolution models, or even more complex galaxy formation models. In the latter case also geometrical inputs are provided.

• The pure stellar integrated SED can be obtained straightforwardly by making use of a library of SSP covering a large range in age and metallicity (e.g. Bressan et al. 1998, 2002; Bruzual & Charlot 2003, 2008; Maraston 2005; Buzzoni 1995, 2002). Then the spectral luminosity is obtained as a sum of that of the different stellar generations weighted by the SFR at their birth, i.e.

$$L_\lambda(T) = \int_0^T L_\lambda^{\rm SSP}(T-t, Z(t))\, {\rm SFR}(t)\, dt\,,$$

or more in general

$$L_\lambda(T) = \int_0^T \int_0^1 L_\lambda^{\rm SSP}(T-t, Z)\, {\rm SFR}(t, Z)\, dZ\, dt\,,$$

which applies for instance for galaxy mergers that will not give rise to a one to one relation between age and metallicity as instead is the case for a "monolithic" evolution.

• The way in which the interaction between stellar radiation and dust in the ISM is accounted for to evaluate UV/optical attenuation and IR emission from dust can be broadly classified into two main approaches, semi-empirical and theoretical:

- **Semi-empirical:** In this case one typically adopts an attenuation curve (a wavelength dependence of the attenuation such as e.g. the Calzetti (2000) or the Charlot & Fall (2000) curves, or an extinction curve with a slab geometry, with a normalization in a given band). This provides the total amount of IR luminosity. The spectral shape of $L_{\rm IR}$ is usually obtained by adopting modified black-body curves or the superposition of templates with different relative normalization. These shapes are adjusted by comparing with observed IR relations (e.g. IRAS and Spitzer color-color or color-luminosity plots). This kind of approach is particularly useful for statistical analysis of large data sets of nearby galaxies, requiring fast computations. On the other hand, they have not a great predictive power, so caution must be paid when applying them to interpret objects for which they have not been calibrated for, such as high-z galaxies (e.g. Devriendt, Guiderdoni, & Sadat 1999; Chary & Elbaz 2001; Dale et al. 2001; Dale & Helou 2002; Galliano et al. 2003; Lagache, Dole, & Puget 2003; Da Cunha, Charlot, & Elbaz 2008).

- **Theoretical:** Theoretical models include an explicit computation of the radiative transfer (RT) and of the dust emission, at different levels of complexities, ingredients and approximations depending on the aims. This requires the adoption of a geometry for stars and dust (bulge, disk, clumps, diffuse etc), of a dust model (dust grains composition, optical properties, size distribution), and the computation of the temperature of dust as a function of the incident radiation field for each type of grain. The RT of the radiation through the dust distribution is usually solved either with ray-tracing (direct solution of the RT equation) or Monte Carlo (following the path of randomly-generated photons) methods. These models allow a broad interpretative and predictive power, their major drawback being the required computing time. For some applications (e.g. the simulation of large number of galaxies in cosmological volumes) the computing time is too demanding. Models in this group include Rowan-Robinson (1980); Rowan-Robinson & Crawford (1989); Silva et al. (1998); Efstathiou & Rowan-Robinson (2003); Takagi, Arimoto, & Hanami (2003); Takagi, Vansevicius, & Arimoto (2003); Siebenmorgen & Krugel (2007); Dopita et al. (2005, 2006a,b); Groves et al. (2008); Popescu et al. (2000); Tuffs et al. (2004); Gordon et al. (2001); Baes et al. (2003); Jonsson (2006); Bianchi (2008); Chakrabarti et al. (2008); Li et al. (2008).

In § 2 I summarize the main characteristics and aims of `GRASIL`, the code we developed to model the SED of galaxies from the UV to the radio range by treating the reprocessing of stellar radiation by dust with particular care. The model has been widely applied both to interpret observed SEDs of galaxies of different types to retrieve information on the SF history, masses of stars and gas, attenuation properties etc., and to compute SEDs for different galaxy

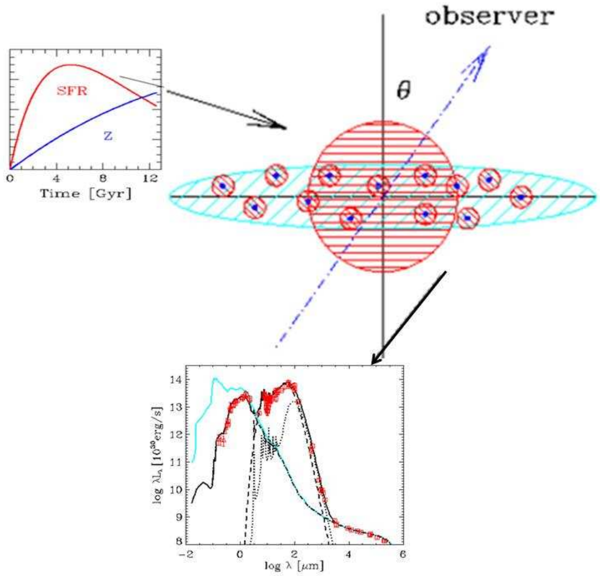

Fig. 3. Scheme for GRASIL: the stellar populations and mass of gas given in input to GRASIL are subdivided into star-forming optically thick molecular clouds hosting the youngest stars and the diffuse medium associated with more evolved stars. Stars and dust are arranged in a bulge and/or in a disc, by making use, when available, of the geometrical information provided by the input model galaxy. The radiative transfer of the radiation through the dust distribution and the dust emission at each point of the galaxy is computed to yield the emerging SED (UV to radio) along any line of sight.

formation models in the cosmological context. In § 3 some applications of GRASIL to semi-analytical galaxy formation models is summarized. The main problem encountered when properly modelling SEDs for galaxies in simulated cosmological volumes is the computing time. For this reason, and anyway for any application requiring large numbers of models, in § 4 I describe the implementation of the artificial neural network algorithm to compute SEDs. This allows to solve the computing time problem and therefore to rely on a realistic modelling of the SEDs also to simulate large cosmological volumes.

2. MODELLING SEDS WITH GRA(PHITE)SIL(ICATE)

For a general purpose modelling of galaxy SEDs we developed the code GRASIL[2] (Silva et al. 1998, hereafter S98; Silva 1999, hereafter S99; Granato et al. 2000; Bressan, Silva, & Granato 2002; Silva et al. 2003; Panuzzo et al. 2003; Vega et al. 2005). Our main aims were to have a relatively realistic and flexible multi-wavelength model with a reasonable computing time, that could be applied both to interpret observations and to make predictions for galaxy formation models. These requirements drove our choices for the ingredients and computations to include in GRASIL (see Figure 3 for a scheme). To fulfill the first requirement we consider:

- A relatively realistic geometry with stars and dust in a bulge and/or in a disk, by adopting a King and a double exponential profile respectively.
- Three different dusty environments: a dense phase to represent star forming molecular clouds (MC) associated with the youngest stars, a diffuse phase (the "cirrus") associated with more evolved stars, and the dusty envelopes around AGB stars. Therefore we take into account the clumping of both (young) stars and dust within a more diffuse medium. The relative importance of the different phases depends on the star formation history.
- We account for the birth of stars within MCs by gradually decreasing the fraction of energy they emit within MCs as a function of their age. This gives rise to an age-dependent extinction that can have important properties when interpreting observations.
- The dust grains include big grains in thermal equilibrium with the radiation field, very small grains fluctuating in T, and PAH molecules. The emission from each type of grain is computed as a function of the radiation field in each volume element of the model galaxy.
- We include (directly in the SSPs) the computation of the radio emission, both thermal and non-thermal, adding further insights to interpret observations.
- The output consists in the UV to radio SED, both continuum and nebular lines.

To fulfill the computing time requirement, the model has geometrical symmetries (axial and equatorial), we approximate the RT in the cirrus component (the real bottle-neck of the whole computation), and we avoid Monte Carlo calculations. See S98 and S99 for more details.

Several improvements and updates have been performed since the first version in S98. These comprise: (1) the inclusion of radio emission (Bressan et al. 2002); (2) the nebular emission lines (Panuzzo et al. 2003); (3) the computation of the PAH bands has been updated by adopting the Draine & Li (2007) cross sections and profiles, following the procedure described in Vega et al. (2005) for the Li & Draine (2001) version; (4) the setting of the grids (reported in appendix A of S99) have been improved

[2] http://adlibitum.oat.ts.astro.it/silva/default.html.

so that also very high optical depths ($\tau_{1\mu m} \sim 100$) in the cirrus can be managed; (5) the usage has been made easier through the user-friendly web interface `GALSYNTH`[3] that allows to run `GRASIL` (and the chemical evolution code `CHE_EVO` to produce the input star formation histories) with an on-line help and without installing the code; (6) if required, the computing time has been improved by more than 2 orders of magnitude with the ANN algorithm (see § 4).

With these ingredients the model has been successfully applied in many contexts (e.g. see the above references and Granato et al. 2004; Silva et al. 2005; Panuzzo et al. 2007a,b; Fontanot et al. 2007; Galliano et al. 2008; Vega et al. 2008; Baugh et al. 2005; Lacey et al. 2008; Fontanot et al. 2009; Schurer et al. 2009).

As an example of interpretative work, Figure 4 shows a full SED fit to NGC 4435, an early-type galaxy in the Virgo cluster for which we obtained Spitzer/IRS data (Bressan et al. 2006). The model fit allowed us to estimate several quantities such as the mass of stars and dust and the age of the last burst. The estimated values are consistent with independent evaluations from emission lines and dynamical studies (see Panuzzo et al. 2007b). Other interpretative works include for instance studies of the UV attenuation properties in spiral galaxies and the role played by the age-dependent attenuation (Granato et al. 2000; Panuzzo et al. 2007a); detailed analysis of the star formation rates, masses and staburst/AGN contributions in ULIRGs (Vega et al. 2008, and this volume); exploiting the IR and radio SEDs to date starburst galaxies (Bressan et al. 2002); studying and quantifying the effects of the chemical evolution of dust on the SED (Schurer et al. 2009); assigning an age and a mass to super star clusters (Galliano et al. 2008).

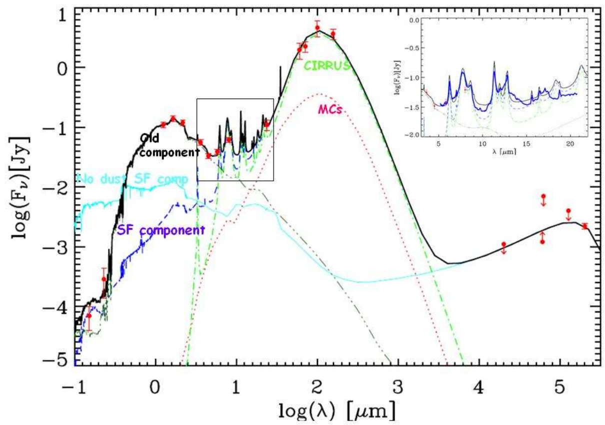

Fig. 4. Fit to the observed SED of NGC4435, an early-type galaxies in the Virgo cluster for which we obtained Spitzer/IRS spectra (in the inset). The different components contributing to the model SED are indicated in the figure. From Panuzzo et al. (2007b).

3. COMPUTING SEDS IN SEMI-ANALYTICAL GALAXY FORMATION MODELS

The study of galaxy formation and evolution is being heavily tackled in these years both observationally and theoretically. Observational programs covering the whole wavelength range are systematically and directly unveiling galaxy populations at all redshifts, whose main properties depend on the selection criteria. The detection of high-z galaxy populations are particularly important to track the process of galaxy formation as a function of the cosmic epoch.

From the theoretical point of view, the modeling of galaxy formation and evolution in a cosmological context involves many processes at very different scales, from Mpcs to sub-pc. The widest range of observed galaxy properties have been analyzed using the so-called semi-analytic methods (White & Rees 1978; Lacey & Silk 1991; White & Frenk 1991), that consist in calculating the evolution of the baryon component using simple analytical expressions, while the evolution of the dark matter (DM) is calculated directly using gravity-only N-body or Monte Carlo techniques. Also hydro-simulations must include sub-grid analytical expressions for fundamental processes such as SF and feedback, shaping the final result (e.g. Di Matteo, Springel, & Hernquist 2005).

The final step to get the output simulated galaxy catalogues, is the computation of the full range SED of each mock galaxy, *by appropriately taking into account its particular star formation and metallicity history and geometrical arrangement of the stellar populations and of the ISM, as predicted by the model, so to check that the predictions are or are not representative of the real universe* and retrieve some information on the galaxy formation. The best way to proceed would be a full Monte Carlo RT code to allow any geometrical configuration of the distribution of the stars and of the ISM. Of course this is not feasible because of diverging computing times. This is not possible also if one were to consider only the optical-UV extinction and avoiding the computation of the IR emission (thus avoiding the comparison with a large dataset). In fact, RT Monte Carlo codes at present are used coupled with hydro-simulations of single galaxies, not for cosmological applications

[3] `http://galsynth.oapd.inaf.it/galsynth/`.

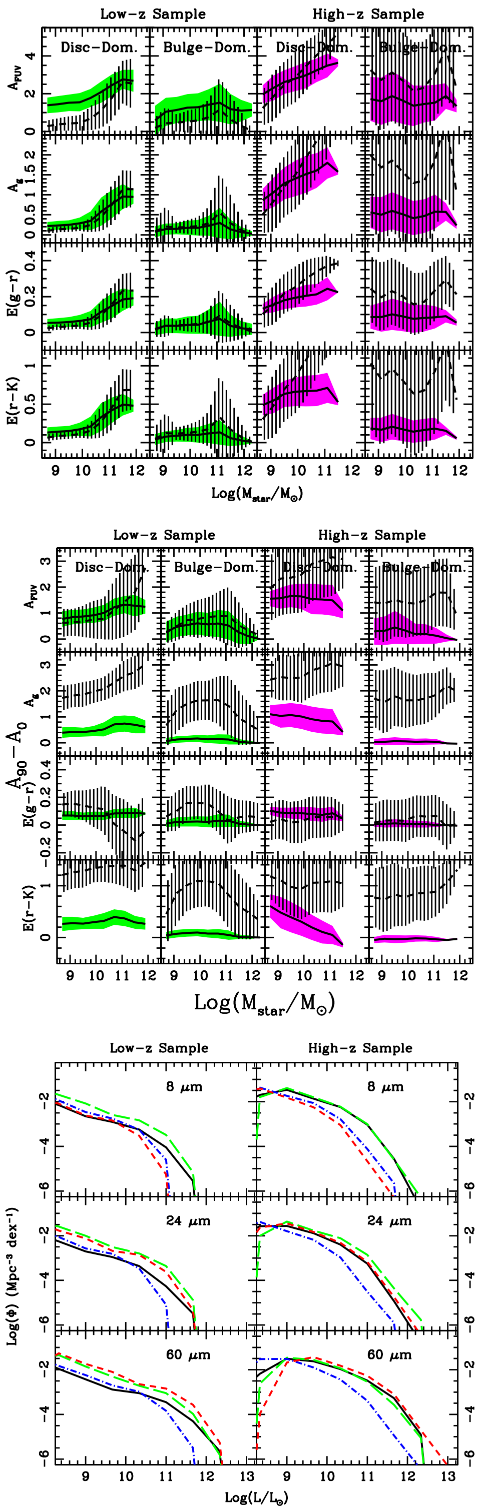

Fig. 5. Attenuations and LFs for a low and a high-z galaxy catalogue from MORGANA. SEDs computed with GRASIL (continuous regions and lines) and with semi-empirical treatments (hatched regions and dashed lines). See text for details.

(e.g. Jonsson et al. 2006; Chakrabarti et al. 2007; Li et al. 2008). On the other hand, since the attempt to theoretically understand the assembly of baryons within the hierarchy of DM halos is inevitably subjected to strong uncertainties and degeneracies, as much observational constraints as possible must be taken into account by models to hope to get some hints on the overall scenario and possibly the main involved physical processes, therefore only a multi-wavelength analysis of galaxy data can help to understand the complexities of galaxy formation and evolution.

Most semi-analytical models (SAM) have made use of simple empirical treatments to compute the SED (e.g. Guiderdoni et al. 1998; Kauffmann et al. 1999; Somerville & Primack 1999; Hatton et al. 2003; Blaizot et al. 2004; De Lucia, Kauffmann, & White 2004).

The only SAMs that include a UV to sub-mm RT computation are GALFORM (Cole et al. 2000; Granato et al. 2000; Baugh et al. 2005; Lacey et al. 2008), MORGANA (MOdel for the Rise of GAlaxies aNd Active nuclei, Monaco et al. 2007; Fontanot et al. 2007, 2009), and ABC (Anti-hierarchical Baryonic Collapse, Granato et al. 2004; Silva et al. 2005; Lapi et al. 2006).

In particular, GALFORM was the first SAM for which a detailed comparison with UV to sub-mm data, both at low and high-z, was undertaken. It was constrained by considering a large wealth of observations, including spectral properties of galaxies as a function of their morphology, attenuation and inclination-dependent properties, luminosity functions, galaxy counts and redshift distributions. Only by being able to consider in a reliable way such a large wavelength range it was possible to find out strong constraints to the galaxy model (see Baugh et al. 2005).

The computing time is probably the main reason why the importance of the reliability of the treatment of the SED has been very often overlooked, apart maybe an underestimation of the importance of dust effects until a few years ago. In fact, at least for SAMs, the time required by the RT calculation is the bottleneck of the whole computation.

An interesting –although obvious– point to take into account when computing SEDs, is that different treatments yield different SEDs for the same input star formation history. Therefore the interpretation of the predictions of a galaxy formation model and claims on its successes or failures are affected by the SED computation. As an example, in Figure 5 we show the attenuation properties and the IR luminos-

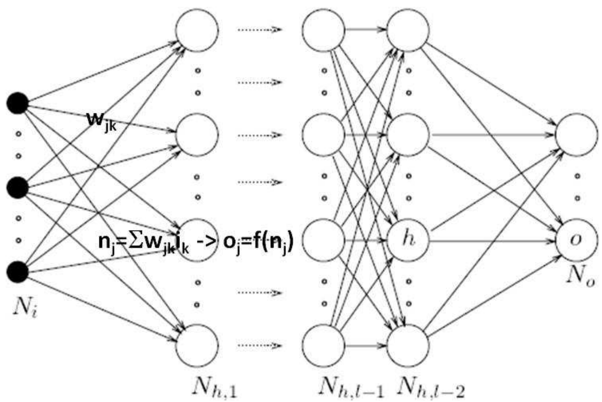

Fig. 6. Schematic representation of a feed-forward multi-layer ANN: a network of connected computing units ("neurons"), with a set of input units (in our case the controlling parameters of the SED), and a set of output units (in our case the SED, one unit for each λ). The weights (strengths) of the connections between each couple of units of consecutive layers are the adjustable parameters of the ANN. This is accomplished by training the ANN to reproduce a large set of pre-computed inputs (SED controlling parameters)-outputs (corresponding SED). See text for more details.

ity functions (LF) we obtain for a low and a high-z mock catalogue extracted from the `MORGANA` model, by computing SEDs either with `GRASIL` or with semi-empirical treatments. The upper panel shows attenuations and color excesses; the middle panel edge-on to face-on attenuation; the bottom panel the IR LFs (see more details in Fontanot et al. 2009).

4. MODELLING SEDS WITH ARTIFICIAL NEURAL NETWORKS

4.1. *Generalities*

SEDs are complex, non-linear, high-dimensional and large-variance functions of some galaxy properties. Artificial neural networks (ANN) are mathematical algorithms particularly suited to handle this kind of complex function approximation. They were introduced to somehow replicate the brain behavior, in particular their strength is that they are constructed so to *learn from examples*. As shown below, actually we have chosen ANN to model SEDs because they work.

A typical scheme of how ANN work is in Figure 6:

• The algorithm is based on a group of computing units ("neurons") connected in a network, with a set of input units (in our case the parameters determining the SED), and a set of output units (in our case the SED, one unit for each λ). The way in which the inputs are transmitted and elaborated to reconstruct the output is set according to the architecture, the propagation rule, and the learning algorithm.

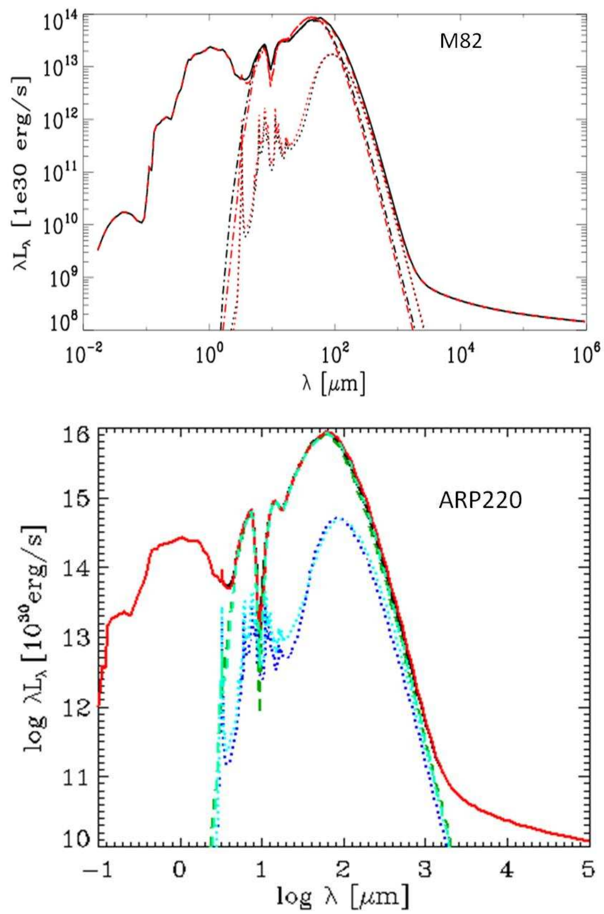

Fig. 7. Examples of SEDs computed with "full" `GRASIL` compared to their reconstruction with the ANN method. The SEDs are almost superimposed.

• The architecture is the pattern of connection between the units and the way in which data are propagated. We adopt a typical *feed-forward multi-layer* ANN. This means that, between the input and output layers, there is at least one hidden layer of computing units, and the signal moves only in the forward direction, each unit of one layer being connected to all units of the next layer.

• The propagation rule is such that the signal moves in parallel, the operation made by each unit is a weighted sum of the signal received by all units of the previous layer, i.e. $n_j = \sum_k w_{jk}\, i_k$, where w_{jk} is the value of the connection between the destination unit j and the original unit k of the previous layer. Then the actual output value from unit j is obtained by operating a non-linear function on it, i.e. $o_j = f(n_j)$. A typical choice for $f(x)$ is the sigmoid function.

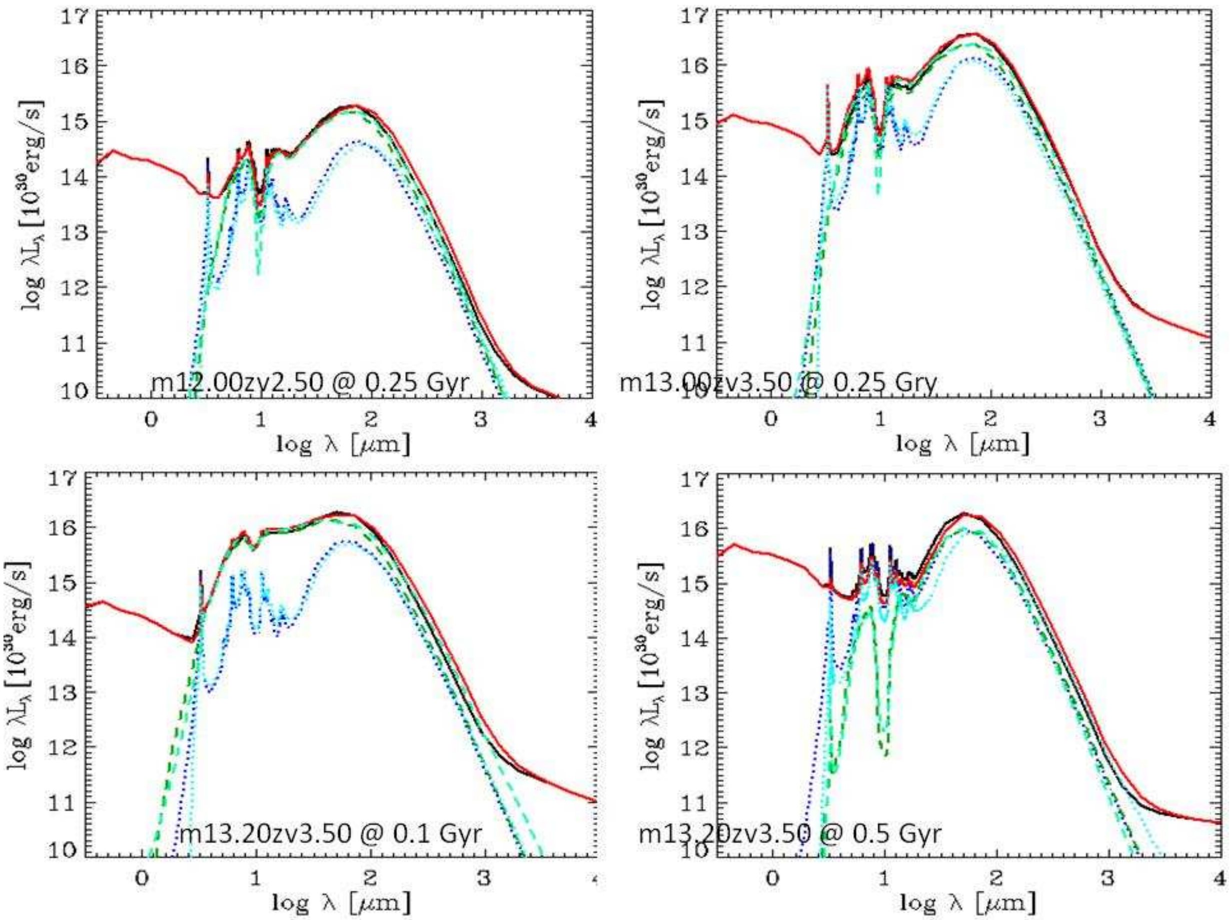

Fig. 8. Examples of randomly extracted galaxy models from the ABC SAM. The SEDs obtained either with the full GRASIL or the ANN reconstruction are almost superimposed.

• The learning or training algorithm we have adopted is the *supervised* one, in which the ANN is trained with a given target. The weights are adjusted to best approximate a given set of known inputs/outputs. This means the ANN is trained to predict the SED from controlling parameters using a suitable pre-computed training set of input parameters and their corresponding SEDs. The best values of the weights are then used to reconstruct the SED corresponding to any given set of input parameters.

4.2. *ANN and SEDs*

We have worked to use ANN to compute SEDs with two methods:

• "Universal" and very fast method (Silva et al., in preparation): we have implemented the ANN algorithm directly in GRASIL so that to it is possible to choose the "full mode" or the "ANN mode" to compute the SED. This is possible because in this method the input parameters are those quantities that effectively determine the SED in GRASIL, separately for the star-forming molecular clouds and cirrus components. In the ANN mode, the code computes the extinction normally, while the IR SED is reconstructed with separately trained ANNs for MCs and cirrus, since they have very different properties. This method requires one single trained net (for each component) for any application. Of course the trained net must be suitably set to encompass a large range parameters values.

The controlling parameters for the IR SEDs of MCs are: $\tau_{\rm MC}$ (optical depth of MCs); $\rm R_{MC}/\it R_{\rm subl}$ (the radius of the MC with respect to the dust sublimation radius).

The controlling parameters for the IR SEDs of cirrus are: $\rm L_{dust}$ (bolometric L of cirrus dust); $\rm M_{dust}$ (mass of cirrus dust); τ_p, τ_e (polar and equatorial optical depths of cirrus dust); $\rm r_{star}/r_{dust}$, $\rm z_{star}/r_{star}$, $\rm z_{dust}/r_{dust}$ (scale-radii and scale-heights of stars and dust in the bulge and/or disk); hardness of the radi-

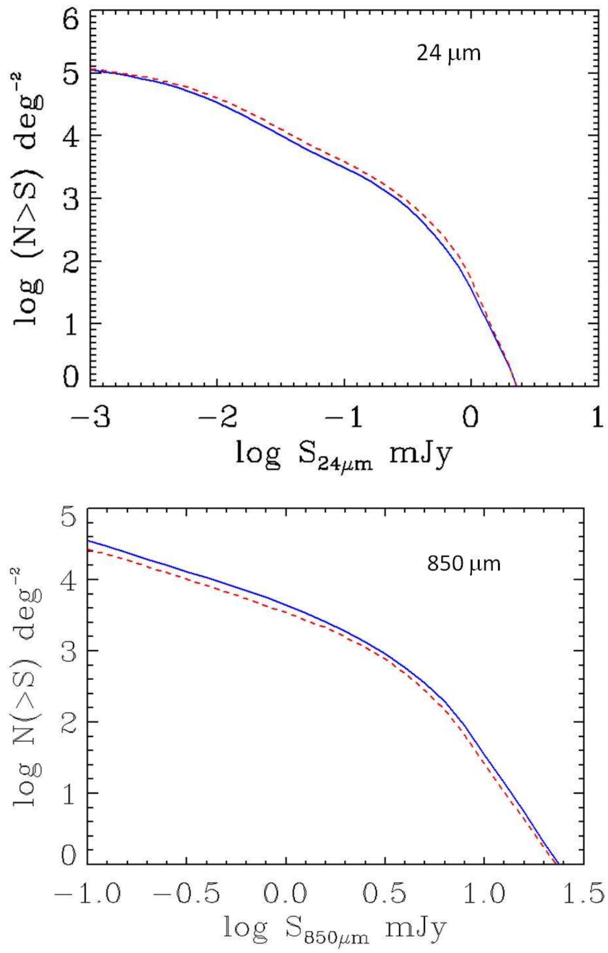

Fig. 9. Galaxy counts at 24 and 850 μm for the ABC SAM: comparison between counts obtained with the full computation for the SED (dashed line), and the ANN reconstruction (continuous line).

ation field heating the cirrus (expressed as the ratio between 0.3 and 1 μm).
The computing time in a ~ 1 GHz CPU is ~ 1 second. This allows large cosmological volumes to be simulated.

• "Less Universal" and super fast method (Almeida et al., in preparation): this method has been specifically studied for the GALFORM+GRASIL model to be used within the Millennium Simulation. The input parameters are searched among the GALFORM galaxy properties, and include the stellar mass and metallicity, the circular velocity, the bolometric luminosity, the half-mass radii for bulge and disk, the V-band optical depth, the mass of stars formed in bursts, the time from the last burst. Each new simulated catalogue of galaxies requires its own trained net. The computing time with this method is extremely fast, $\ll 1$ sec. It therefore allows to fully exploit the whole Millennium Simulation.

Figures 7 and 8 show examples of SEDs reconstructed with the ANN method compared with the corresponding original SEDs computed directly with GRASIL. The first plot shows the models fitting the observed SEDs of the well-known starburst M82 and the ultra-luminous IR galaxy ARP220. The second plot show examples of randomly extracted galaxy models from the ABC semi-analytical galaxy formation model. In either case the reconstructed SED is almost superimposed to the original one, with differences amounting to a few percents ($< 10\%$). More integrated quantities, such as luminosity functions and galaxy counts, are therefore expected to provide even better results, since small differences in the SEDs are smoothed out. As an example, Figure 9 shows the comparison for the 24 and 850 μm galaxy counts for the ABC model.

I am grateful to the organizers for their kind invitation. The work presented in this contribution is the result of long standing collaborations in particular with Carlton Baugh, Alessandro Bressan, Carlos Frenk, Fabio Fontanot, Gian Luigi Granato, Cedric Lacey, Pierluigi Monaco, Pasquale Panuzzo, Olga Vega. I acknowledge financial support by INAF and INAOE.

REFERENCES

Baugh, C. M., Lacey, C. G., Frenk, C. S., Granato, G. L., Silva, L., Bressan, A., Benson, A. J., & Cole, S. 2005, MNRAS, 356, 1191
Bianchi, S. 2008, A&A, 490, 461
Blaizot, J., Guiderdoni, B., Devriendt, J. E. G., Bouchet, F. R., Hatton, S. J., & Stoehr, F. 2004, MNRAS, 352, 571
Bressan, A., Granato, G. L., & Silva, L. 1998, A&A, 332, 135
Bressan, A., Silva, L., & Granato, G. L. 2002, A&A, 392, 377
Bressan, A., et al. 2006, ApJ, 639, 55
Bruzual, G., & Charlot, S. 2003, MNRAS, 344, 1000
Buzzoni, A. 1995, ApJS, 98, 69
_________. 2002, AJ, 123, 1188
Calzetti, D., Armus, L., Bohlin, R. C., Kinney, A. L., Koorneff, J., & Storchi-Bergmann, T. 2000, ApJ, 533, 682
Chakrabart, S., Fenner, Y., Cox, T. J., Hernquist, L., & Whitney, B. A. 2008, ApJ, 688, 972
Charlot, S., & Fall, S. M. 2000, ApJ, 539, 718
Chary, R., & Elbaz, D. 2001, ApJ, 556, 562
Cole, S., Lacey, C. G., Baugh, C. M., & Frenk, C. S. 2000, MNRAS, 319, 168

Da Cunha, E., Charlot, S., & Elbaz, D. 2008, 388, 1595
Dale, D., & Helou, G. 2002, ApJ, 576, 159
Dale, D., et al. 2001, ApJ, 549, 215
Devriendt, J. E. G., Guiderdoni, B., & Sadat, R. 1999, A&A, 350, 381
Di Matteo, T., Springel, V., & Hernquist, L. 2005, Nature, 433, 604
Dopita, M. A., et al. 2006a, ApJ, 647, 244
Dopita, M. A., et al. 2006b, ApJS, 167, 177
Dorschner, J., & Henning, T. 1995, A&A Rev., 6, 271
Draine, B. T. 2003, ApJ, 598, 1017
Draine, B. T., & Li, A. 2007, ApJ, 657, 810
Fontanot, F., Monaco, P., Silva, L., & Grazian, A. 2007, MNRAS, 382, 903
Fontanot, F., Somerville, R. S., Silva, L., Monaco, P., & Skibba, R. 2009, MNRAS, 392, 553
Galliano, E., et al. 2008, A&A, 492, 3
Gordon, K. D., Misselt, K. A., Witt, A. N., & Clayton, G. C. 2001, ApJ, 551, 269
Granato, G. L., De Zotti, G., Silva, L., Bressan, A., & Danese, L. 2004, ApJ, 600, 580
Granato, G. L., et al. 2000, ApJ, 542, 710
Groves, B., et al. 2008, ApJS, 176, 438
Guiderdoni, B., Hivon, E., Bouchet, F. R., & Maffei, B. 1998, MNRAS, 295, 877
Hatton, S., Devriendt, J., Ninin, S., Bouchet, F. R., Guiderdoni, B., & Vibert, D. 2003, MNRAS, 343, 75
Jonsson, P. 2006, MNRAS, 372, 2
Kauffmann, G., Colberg, J. M., Diaferio, A., & White, S. D. M. 1999, MNRAS, 303, 188
Lacey, C. G., Baugh, C. M., Frenk, C. S., Silva, L., Granato, G. L., & Bressan, A. 2008, MNRAS, 385, 1155
Lacey, C. G., & Silk, J. 1991, ApJ, 381, 14
Lagache, G., Dole, H., & Puget, J. L. 2003, MNRAS, 338, 555
Lapi, A., Shankar, F., Mao, J., Granato, G. L., Silva, L., De Zotti, G., & Danese, L. 2006, ApJ, 650, 42
Li, A., & Draine, B. T. 2001, ApJ, 554, 778
Li, Y., et al. 2008, ApJ, 678, 41
Maraston, C. 2005, MNRAS, 362, 799
Mathis, J. S. 1990, ARA&A, 28, 37
Monaco, P., Fontanot, F., & Taffoni, G. 2007, MNRAS, 375, 1189
Panuzzo, P., Bressan, A., Granato, G. L., Silva, L., & Danese, L. 2003, A&A, 409, 99
Panuzzo, P., Granato, G. L., Buat, V., Inoue, A. K., Silva, L., Iglesias-Paramo, J., & Bressan, A. 2007a, MNRAS, 375, 640
Panuzzo, P., Vega, O., Bressan, A., Buson, L., Clemens, M., Rampazzo, R., Silva, L., Valdes, J. R., & Granato, G. L. 2007b, ApJ, 656, 206
Popescu, C. C., Misiriotis, A., Kylafis, N. D., Tuffs, R. J., & Fischera, J. 2000, A&A, 362, 138
Rowan-Robinson, M. 1980, ApJS, 44, 403
Rowan-Robinson, M., & Crawford, J. 1989, MNRAS, 238, 523
Schurer, A., Calura, F., Silva, L., Pipino, A., Granato, G. L., Matteucci, F., & Maiolino, R. 2009, MNRAS, 394, 2001
Siebenmorgen, R., & Krugel, E. 2007, A&A, 461, 445
Silva, L., Granato, G. L., Bressan, A., & Danese, L. 1998, ApJ, 509, 103 (S98)
Silva, L. 1999, PhD Thesis, SISSA, Trieste (S99)
Silva, L., De Zotti, G., Granato, G. L., Maiolino, R., & Danese, L. 2005, MNRAS, 357, 1295
Somerville, R. S., & Primack, J. R. 1999, MNRAS, 310, 1087
Takagi, T., Arimoto, N., & Hanami, H. 2003, MNRAS, 340, 813
Takagi, T., Vansevicius, V., & Arimoto, N. 2003, PASJ, 55, 385
Tuffs, R. J., Popescu, C. C., Volk, H. J., Kylafis, N. D., & Dopita, M. A. 2004, A&A, 419, 821
Vega, O., Silva, L., Panuzzo, P., Bressan, A., Granato, G. L., & Chavez, M. 2005, MNRAS, 364, 1286
Vega, O., Clemens, M. S., Bressan, A., Granato, G. L., Silva, L., & Panuzzo, P. 2008, A&A, 484, 631
White, S. D. M., & Frenk, C. S. 1991, ApJ, 379, 52
White, S. D. M., & Rees, M. J. 1978, MNRAS, 183, 341